J Neurophysiol 104: 2985–2994, 2010.
First published September 8, 2010; doi:10.1152/jn.00483.2010.

The Central Nervous System Does Not Minimize Energy Cost in Arm Movements

Dinant A. Kistemaker, Jeremy D. Wong, and Paul L. Gribble
Social Science Centre, The University of Western Ontario, London, Ontario, Canada

Submitted 28 May 2010; accepted in final form 7 September 2010

Kistemaker DA, Wong JD, Gribble PL. The central nervous system does not minimize energy cost in arm movements. *J Neurophysiol* 104: 2985–2994, 2010. First published September 8, 2010; doi:10.1152/jn.00483.2010. It has been widely suggested that the many degrees of freedom of the musculoskeletal system may be exploited by the CNS to minimize energy cost. We tested this idea by having subjects making point-to-point movements while grasping a robotic manipulandum. The robot created a force field chosen such that the minimal energy hand path for reaching movements differed substantially from those observed in a null field. The results show that after extended exposure to the force field, subjects continued to move exactly as they did in the null field and thus used substantially more energy than needed. Even after practicing to move along the minimal energy path, subjects did not adapt their freely chosen hand paths to reduce energy expenditure. The results of this study indicate that for point-to-point arm movements minimization of energy cost is not a dominant factor that influences how the CNS arrives at kinematics and associated muscle activation patterns.

INTRODUCTION

A fundamental question in motor control is how the CNS coordinates the many kinematic and mechanical degrees of freedom of the body to control posture and movement (Bernstein 1967). Several theories of motor control are based on or inspired by the idea that the CNS arrives at a set of muscle activation patterns for a given task by minimizing a cost function in which minimization of energy cost takes part (e.g., Alexander 1997; Cruse 1986; Engelbrecht 2001; Hatze and Buys 1977; Kashima and Isurugi 1998; Nelson 1983; Rasmussen et al. 2001; Soechting et al. 1995; Todorov 2004; Todorov and Jordan 2002; Torres and Zipser 2002). Such theories have been shown to predict kinematic features for movement tasks in the absence of external loads, like relatively straight hand paths and bell-shaped velocity profiles. However, at least for unperturbed arm movements, many motor control theories predict these same kinematics (e.g., d'Avella et al. 2006; Flash and Hogan 1985; Uno et al. 1989). In addition, even if kinematics and muscle activation patterns are in accordance with energy minimization, it would not represent evidence that energy cost is minimized by the CNS to generate motor commands. For example, the motor commands that minimize energy cost could have been selected over an evolutionary timescale.

The goal of the present study was to directly test the extent to which energy cost is minimized by the CNS in the context of a motor learning task. One of the most well studied motor learning tasks involves making arm movements while grasping a robotic device that applies forces to the hand that are perpendicular and proportional to the hand velocity (Caithness et al. 2004). Unfortunately, the mechanics of these so-called curl fields are such that the minimal energy path is similar to movements in the absence of forces (see METHODS). Therefore this motor learning task is unsuitable to investigate whether energy minimization plays a role in the selection of kinematics and/or muscle activation patterns by the CNS.

In the present study we designed a novel force field specifically to dissociate the minimal energy path from the relatively straight paths that subjects produce in the absence of forces. Importantly, this force field was constructed such that: *1*) there is a continuous negative energy gradient toward the minimal energy trajectory, *2*) forces applied to the hand never pull or push in the direction of the minimal energy trajectory, and *3*) all possible trajectories are equally stable. Using this force field enabled us to directly test the idea that the CNS incorporates energy cost in motor learning by determining to what extent subjects adapted their movements in the force field to expend less energy.

METHODS

Ethics statement

All subjects reported no history of visual, neurological, or musculoskeletal disorder. Written informed consent was obtained from each subject prior to participation. All procedures were approved by the University of Western Ontario Research Ethics Board.

Experimental setup

Subjects made movements while grasping the handle of an InMotion robotic manipulandum (Interactive Motion Technologies, Cambridge, MA; see Fig. 1*A*). Commanded forces to the robot were adjusted to compensate for position dependence of the robot arm's inertia and to create an isotropic inertial characteristic with a mass of 1 kg. The right arm was supported by a custom-made air sled, which expelled compressed air beneath the sled to minimize surface friction. The subject's arm and the manipulandum were beneath a semisilvered mirror, which reflected images projected by a computer-controlled liquid crystal display (LCD) screen. Visual targets were projected that appeared to lie in the same plane as that of the hand. Positional and force data were sampled at 600 Hz and were filtered afterwards using a fourth-order bidirectional Butterworth filter with a cutoff frequency of 15 Hz. Energy delivered to the robot (E_{ext}) was calculated by

$$E_{ext} = \int_0^T F_r \dot{s} \mathrm{d}t \qquad (1)$$

where F_r represents the forces measured at the robot manipulandum, $\dot{s}$ is the velocity of the hand, and T is the movement time. The maximal

Address for reprint requests and other correspondence: D. A. Kistemaker, University of Western Ontario, Social Science Centre, London, ON, Canada N6G 3A9 (E-mail: dinant.kistemaker@gmail.com).

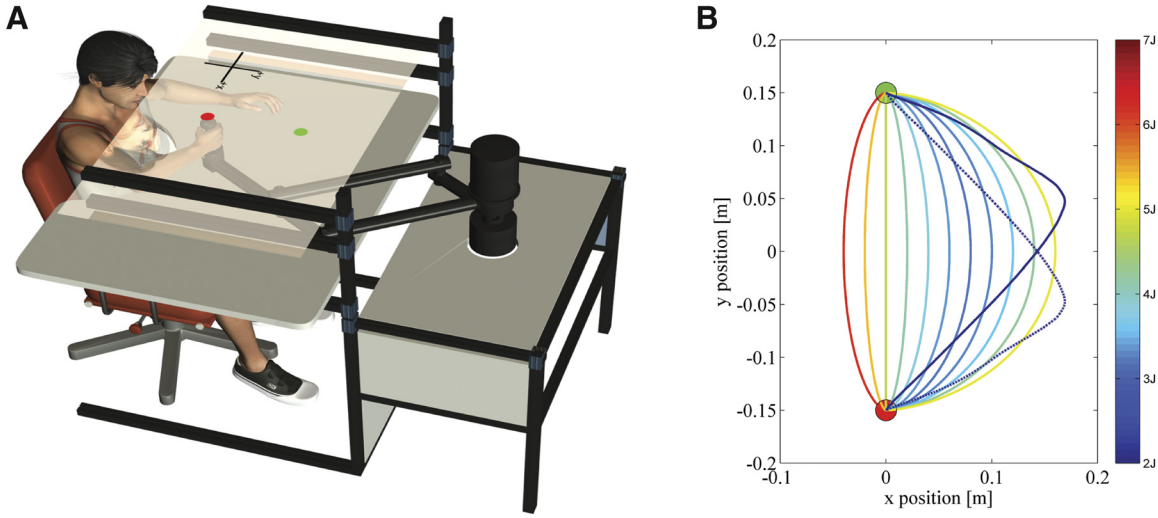

FIG. 1. Experimental setup and minimal energy path. *A*: targets were projected onto a semisilvered mirror using a liquid crystal display monitor suspended 15 cm above the mirror (not shown). Subjects moved from the red start position to the green target position. Two seconds after reaching the target, start and target position were swapped and subjects initiated a new movement. *B*: minimal energy paths (in blue; solid line for outward movements and dashed for inward movements) and the energy required to move along paths with different left–right curvatures at minimal jerk (movement duration: 400 ms). Color coding represents the energy needed to follow a given path and shows that there is a continuous negative energy gradient in the direction of the minimal energy path.

x-deviation was calculated by taking the largest *x*-deviation in either the positive or negative direction between the start and target circle.

Force field

Many studies have used curl fields to study motor learning (e.g., see Caithness et al. 2004). In a curl field, a force is applied at the hand of a subject that scales with and is perpendicular to the hand's velocity. As a consequence, the force applied to the hand does not do work and is a conservative force field. Thus such a force field has a minimal energy trajectory that resembles that of the straight trajectory movements in the null field. To address this issue we designed a novel force field for which the minimum energy path is clearly different from the slightly curved path that subjects produce in the absence of external forces. In this study, the forces delivered to the hand of the subject depended on the *y* position of the hand (y), the *x* and *y* velocities of the hand ($\dot{x}$ and $\dot{y}$), and a constant b (150 Ns/m^2). For outward movements the commanded forces were

$$F_y = b(-\dot{y} + \dot{x}) \cdot |y_{\text{target}} - y| \qquad (2)$$

The force in the *x* direction was always zero. The first component in *Eq. 2* ($-b \cdot y$) produces a pattern of forces such that when a subject is moving straightforward, the robot is delivering a counteracting negative force (see Fig. 2*A*). The second component ($b \cdot x$) results in

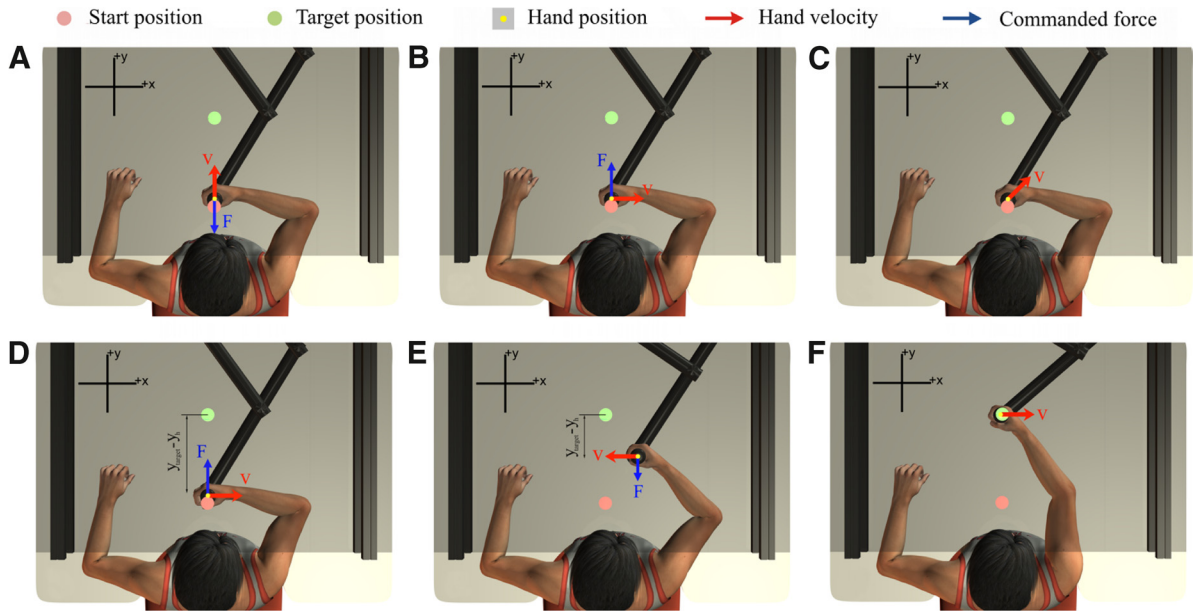

FIG. 2. Explanation of the used force field. *A*: a positive *y* velocity of the hand (red arrow) results in a counteracting negative commanded force (blue arrow). *B*: moving to the right results in an assistive positive force. *C*: moving outward and to the right under exactly 45° results in no commanded force. *D*: moving to the right with a certain speed at the start results in an assistive positive force that is twice as high as a negative counteracting force (*E*) that results from a movement to the left with the *same* speed made halfway between start and target position. *F*: commanded forces at the target are always zero, irrespective of the *x* and *y* velocities of the hand. Note that the preceding explanation is for outward movements. For inward movements, the commanded force for movements in the *x* direction was swapped (compare *Eqs. 2* and *3*).

forces that push the hand forward when the subject is moving to the right (Fig. 2*B*). The summation of the two components ($-\dot{y} + \dot{x}$) results in a forceless condition for movements made under a 45° angle (Fig. 2*C*). The position-dependent component in *Eq. 2* ($|y_{target} - y|$) results in forces applied by the robot that are proportional to the y distance between the hand and target. This ensures that if a subject moves to the right with a certain speed at the start position (Fig. 2*D*), the assisting force is twice as high as the counteracting force when moving to the left, with the same speed halfway between the start and target positions (Fig. 2*E*). In the target position, commanded forces are always zero (Fig. 2*F*), irrespective of the velocity of the hand.

The force field for inward movements was identical for outward movements, except that the direction for the forces in the x direction was swapped

$$F_y = b(-\dot{y} - \dot{x}) \cdot |y_{target} - y| \quad (3)$$

Overall, this force field was organized so that for both outward and inward movements it was energetically beneficial to move to the right at the onset of movement and to move forward and left in a later stage. To provide additional insight in the force field, we calculated the energy required to move the robot through the force field along several (minimal jerk) trajectories with different excursions in the x direction (Fig. 1*B*). All movement durations were 400 ms. Red lines represent high energy cost and blue lines indicate low energy cost. It can be seen that there is a monotonic negative energy gradient toward the minimum.

Figure 1*B* also shows the minimal external energy paths for outward (solid blue line) and inward movements (dashed blue line). These paths are markedly different from the relatively straight hand paths observed in a null field (see RESULTS). Moving along the minimal energy path would therefore require a kinematic detour to the target. Due to the nature of the force field subjects can, but do not need to, move along the minimal energy path to reduce the energy cost of their movement. As explained earlier, the commanded assisting (y) forces for a rightward velocity and the linear scaling of the commanded (y) forces with the distance to the target result in an energetic advantage for any small adjustment of their hand path to the right of those performed in the null field (see also Fig. 1*B*).

Musculoskeletal model and estimation of metabolic energy

The musculoskeletal model of the arm used consisted of three rigid segments interconnected by two hinge joints representing the glenohumeral joint and elbow joint (see also Kistemaker et al. 2006, 2007a). The arm was actuated by six Hill-type muscle units (two monoarticular shoulder and elbow muscles and two biarticular muscles; see Fig. 3*A*). The implemented Hill-type muscle model consisted of a contractile element (*CE*), a series elastic element (*SE*), and a parallel elastic element (*PE*), as shown schematically in Fig. 3*B*. Activation dynamics was added to describe the relation between muscle stimulation (*STIM*) to active state (q). The lengths of the muscle–tendon complexes (l_{MTC}) and moment arms (*arm*) were functions of the joint angles. The musculoskeletal model was extended with a model that allows for the calculation of metabolic energy expenditure (Umberger et al. 2003). This model takes into account energy cost related to the active transport of Ca^{2+}, contractile state (isometric, concentric, and eccentric), and differences in muscle type (parameters taken from Dahmane et al. 2005; Johnson et al. 1973). Detailed descriptions of the musculoskeletal model, energy expenditure model, and how muscle activation patterns were obtained are provided in the APPENDIX.

All data analyses and simulations were run under MATLAB.

Experimental protocol

EXPERIMENT 1. Six right-handed male subjects participated in this experiment. They performed point-to-point movements to visual targets while grasping the handle of the robotic linkage with their right hand. Movements (30 cm) were made toward and away from the body in a horizontal plane along the surface of a desk, at shoulder height (see Fig. 1*A*). The subjects' view of their arm was occluded by the semisilvered mirror. Visual targets were provided on the mirror using an LCD monitor. Only when the participant's hand was within either the start or the target circle, a small dot representing the hand position was plotted. Thus on-line feedback about hand position was provided during the movement. When the target circle was reached, the target changed color to provide feedback indicating that the movement was either well timed (between 300 and 500 ms), too slow, or too fast. To avoid biasing subjects to move along a particular hand path, apart from the timing aspect, no instructions were given as to how the target was to be reached. After 2 s, start and target position were swapped and subjects initiated a new movement toward the original start position. During the first 150 movements, the commanded forces to the robot were zero, hereafter referred to as null field (NF). After that, 300 movements were performed while the robot created a force field (FF), defined by *Eq. 2* and *3*.

EXPERIMENT 2. In a second experiment we investigated the influence of practicing to move along the minimal energy path on the motor behavior of subjects. Another six subjects first made 150 movements in

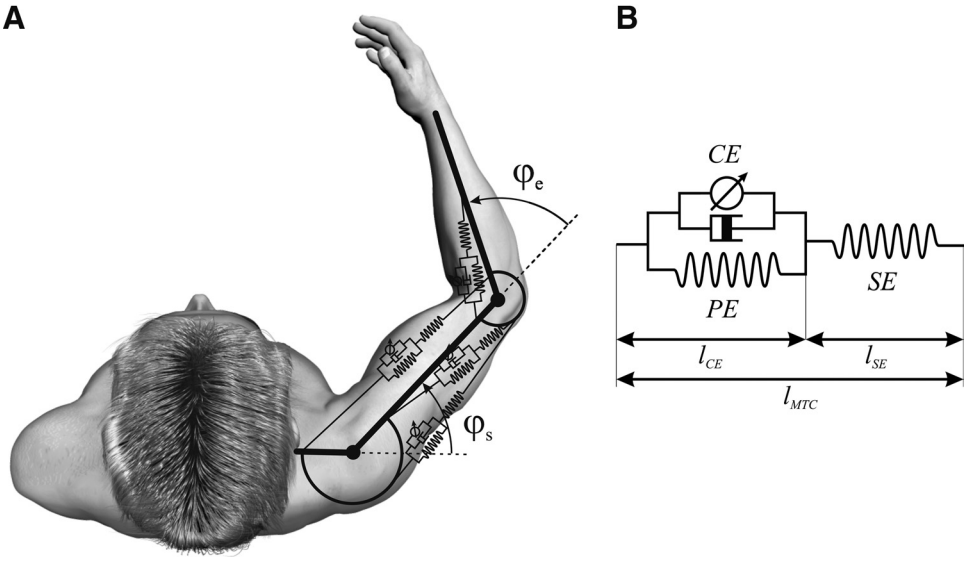

FIG. 3. Schematic drawing of the musculoskeletal model of the arm and Hill-type muscle unit. *A*: φ_e is elbow joint angle and φ_s is shoulder joint angle. *B*: *CE*, contractile element length; l_{CE}, *CE* length; *PE*, parallel elastic element; *SE*, series elastic element; l_{SE}, *SE* length.

the force field. As in *experiment* 1, the visual targets were depicted and the only instruction provided to subjects was to reach the target within the desired time window. After that, we displayed the minimal energy path on the semisilvered mirror and asked subjects to make another 150 movements along this path to the target. In this tracking task only, a small cursor was plotted on the screen representing the subject's hand during the entire movement. As in all conditions, feedback was provided about movement timing by changing the color of the target circle. The subjects were asked to follow the trajectory as accurately as possible, but no feedback was provided as to how well the subject was capable of tracking the minimal energy path. This was done to make the task as simple as possible while experiencing energetically efficient reaching movements. After the tracking task, we removed the minimal energy path (and the feedback of the hand position during the movement) from the display and instructed the subjects to make another 150 movements as they liked. All movements in *experiment* 2 were made in the force field.

EXPERIMENT 3. In a third experiment we tested whether the degree to which subjects reduced energy cost was simply a function of the amount of motor training experienced. We asked two subjects to complete 1,650 movements (>2 h) in the force field. Every 450 movements, subjects were allowed a short rest of 1 min.

RESULTS

Experiment 1

Figure 4*A* shows the average hand paths of subjects for the last 10 trials of 150 trials in the null field and the last of 200 trials in the force field. Movement speeds in the null field and force field were not significantly different (mean peak tangential speed 0.99 m/s in NF, 0.96 m/s in FF, $P = 0.15$, paired *t*-test). It was found that subjects did not change their hand paths (measured as the maximal deviation in the *x* direction) during practice in the force field, but rather continued to move as they did in the null field (mean = −8.0 mm in NF, −8.4 mm at the end of force-field practice, $P = 0.81$, paired *t*-test). Note that even slight changes of their hand path to the right would have reduced the energy cost. Figure 4*B* shows the external energy required for the movements of the subjects in the null field and force field, calculated using kinematic data and the recorded forces in the handle of the robot (see METHODS). A paired *t*-test of the energy required in the first and last 10 successful trials in the force field showed that subjects were not learning to move with less energy over the course of practice in the force field (mean = 5.3 J for first, mean = 5.1 J for last, $P = 0.33$, paired *t*-test). Thus after practicing in the force field subjects moved along the same path as that in the null field and thus used more energy than needed.

Experiment 2

Since the subjects did not learn to move using less energy in the force field, we conducted a second experiment to investigate what would happen after the subjects practiced to move along the minimal energy path. Figure 5*A* shows the average hand paths of the last 10 movements in the three sessions of all successful trials (arrival at target within 300–500 ms). Similarly, Fig. 5*B* shows the average force profiles for all three sessions (in addition to those obtained during the null field session of *experiment* 1). Figure 5*C* shows the external energy delivered to the robot. As can be appreciated from these figures, it was found that before and after practicing to move along the minimal energy path, subjects performed reaching movements as described earlier. Maximum *x*-deviation after practice was not significantly different from that before practice (mean = −6.4 mm before practice, mean = −6.5 mm after practice, $P = 0.42$, paired *t*-test). Moreover, there were no significant differences in the external energy delivered by the subjects before and after practice (mean = 5.1 J before, mean = 5.4 J after, $P = 0.08$, paired *t*-test). Yet, the external energy delivered by the subjects when they were asked to follow the minimal energy path was significantly less (2.7 J; $P < 0.001$) than that when they were free to choose a hand path (5.4 J). Thus even after experiencing hand paths that required significantly less energy to reach the target, subjects moved using more energy when they were free to choose a hand path.

Experiment 3

In a third experiment we examined whether minimization of energy cost simply required more practice in the force field. We asked two subjects to complete 1,650 movements (>2 h) in the force field. Every 450 movements, subjects were allowed a short rest of 1 min. A paired *t*-test showed no significant

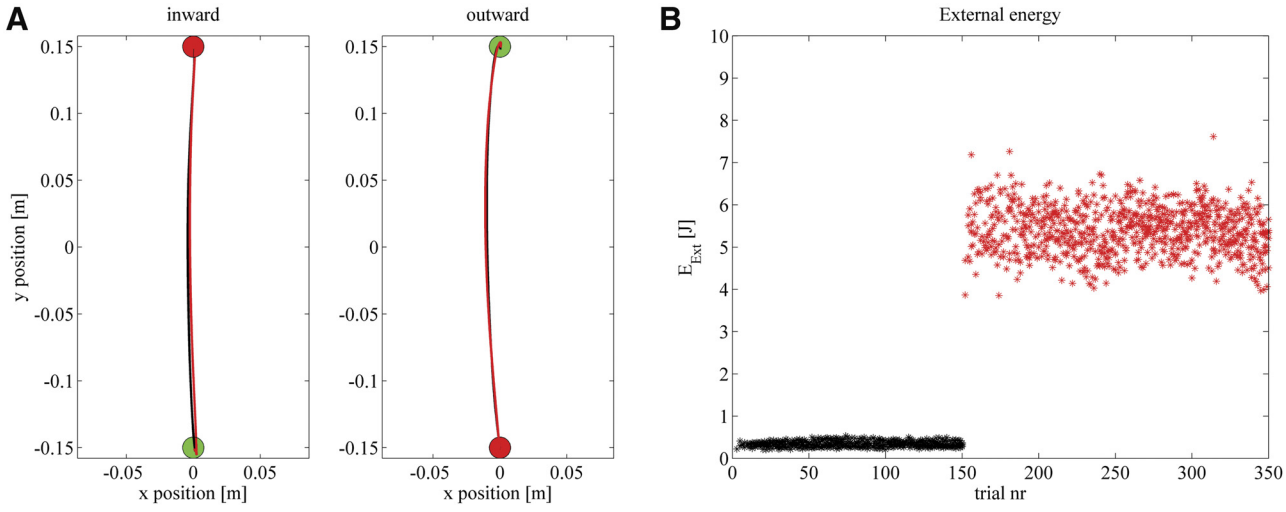

FIG. 4. Average hand paths and required energy per trial in null field and force field. *A*: average hand trajectories of the last 10 trials after null field practice (black) and force field practice. No significant change in hand paths, as measured in maximal deviation in the *x* direction, was observed. *B*: energy per trial for all practice trials meeting the timing criterion (between 300 and 500 ms).

differences in the maximum x-deviation of the first and last 10 movements in the force field (mean = −7.2 mm first, mean = −6.9 mm last, P = 0.31, paired t-test). Thus even after extensive practice in the force field, subjects did not learn to move using less energy.

For an overview of the main statistical findings refer to Table 1.

Arguably, if the CNS minimizes energy it minimizes the total metabolic energy spent by muscles and not external energy. This metabolic energy depends not only on mechanical work done by the muscles (equal to the external energy), but also on several physiological processes within the muscle. To investigate the influence of these factors, we used a detailed musculoskeletal model of the human arm (Kistemaker et al. 2006, 2007b), extended with a model that allows for the calculation of metabolic energy expenditure (Umberger et al. 2003) to simulate the arm movements observed. It was found that for the movements observed in the force field, metabolic energy was mainly determined by the external energy delivered to the robot: the metabolic energy was roughly 4.5-fold the positive work done by the muscles (equivalent to external energy), which is in line with physiological data (Abbate et al. 2002; Zarrugh et al. 1974). The metabolic energy cost in reality can be even higher because the muscle activation patterns of the musculoskeletal model have limited cocontraction of antagonist muscles. To conclude, if subjects did not minimize external energy in the force field, they also did not minimize metabolic energy.

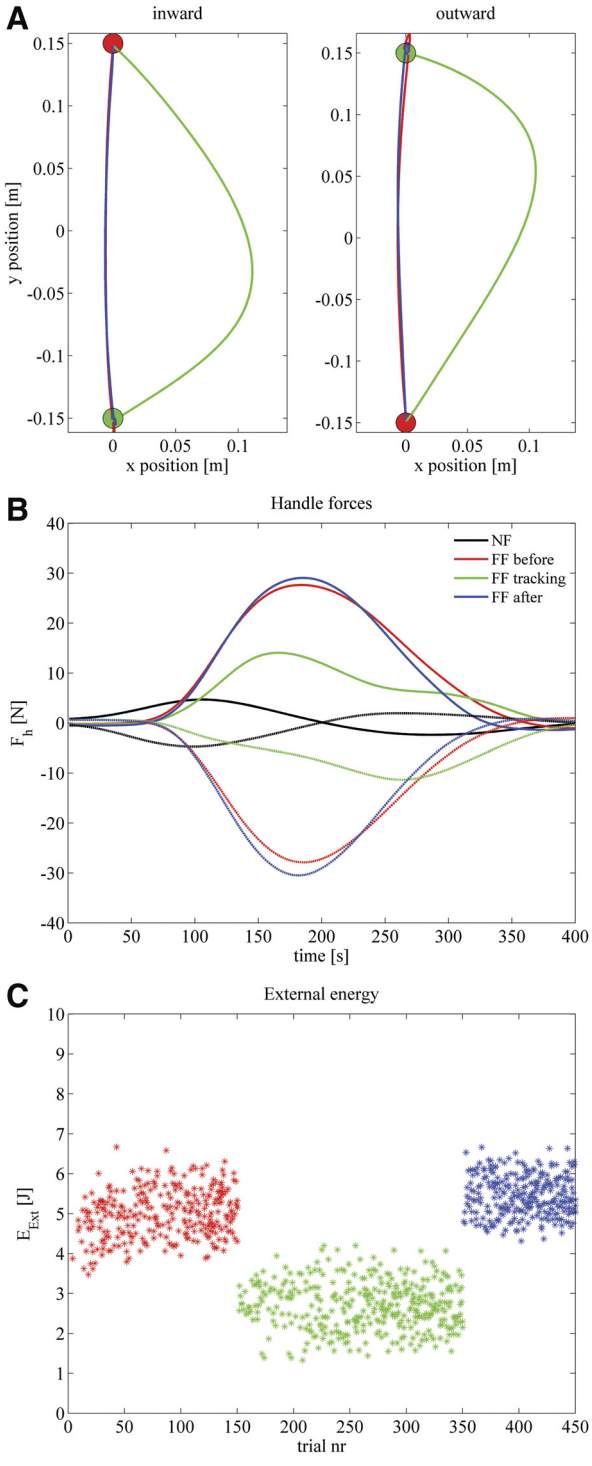

FIG. 5. Average hand paths, force profiles, and required energy per trial before, during, and after training with minimal energy trajectory. *A*: average hand paths of the last 10 of 150 movements that subjects made in the first force field session (red), with the instruction to track the minimal energy path in the force field (green) and in the subsequent session in which again no instructions were given as to how the target had to be reached (blue). No significant differences were found before or after practice with the minimal energy path. *B*: average profiles of the external forces delivered to robot of the last 10 trials in the null field (black) and force field before (red), during (green), and after (blue) training with the minimum energy trajectory. Subjects delivered a peak force of about 7 N to move in the null field and about 36 N in the force field (data were not aligned at peak force, so individual peak forces were somewhat higher). Note that the force patterns in the tracking task were more variable than those in the other tasks. *C*: external energy for all successful trials in the 3 sessions of *experiment* 2. Subjects did not move with less energy after practice with the minimal energy path.

DISCUSSION

Several motor control theories propose that the minimization of energy cost might play an important role in how the CNS arrives at muscle activation patterns and associated kinematics (e.g., Alexander 1997; Cruse 1986; Engelbrecht 2001; Hatze and Buys 1977; Kashima and Isurugi 1998; Nelson 1983; Rasmussen et al. 2001; Soechting et al. 1995; Todorov 2004; Todorov and Jordan 2002; Torres and Zipser 2002). We directly tested this idea by exposing human subjects to a specific force field that has a minimal energy trajectory that is markedly different from those observed in a null field. In addition, the force field was constructed such that there is a continuous negative energy gradient to the minimal energy path. It was found that subjects could quickly learn how to reach in the force field. However, subjects did not adopt hand paths to those requiring less energy, but rather moved just as they did in the null field. Simulations using a detailed model of the human arm showed that metabolic energy was not minimized in the force field. From these results we conclude that minimization of energy is not an important factor that influences how CNS arrives at kinematics and associated muscle activation patterns.

It can be ruled out that a high difficulty in adopting a curved hand path in the force field prevented subjects from adjusting their paths to those requiring less energy. First of all, subjects needed only about 15 trials to adapt to the force field. In

TABLE 1. *Overview of the main statistical results*

Experiment 1	NF_{end}	FF_{begin}	FF_{end}	*P* value
max *x*-dev, mm	−7.10 (±3.5)		−7.60 (±4.2)	0.80
Energy, J		5.49 (±0.49)	5.23 (±0.42)	0.33
Energy, J	0.34 (±0.06)		5.23 (±0.42)	<0.001*
v_{max}, m/s	1.01 (±0.24)		0.99 (±0.37)	0.06
Experiment 2	$FF1_{end}$	FFt_{end}	$FF2_{end}$	
max *x*-dev, mm	−6.50 (±3.6)		−6.10 (±1.2)	0.77
Energy, J	5.00 (±0.58)		5.23 (±0.66)	0.054
Energy, J		2.70 (±0.55)	5.23 (±0.66)	<0.003*
Experiment 3	NF_{end}		FF_{end}	
max *x*-dev, mm	−7.20 (±2.8)		−6.90 (±2.6)	0.31

NF_{end} = average (±SD) of last 10 successful trials in the null field; FF_{begin} = first 10 trials in force field; FF_{end} = last 10 trials in force field; $FF1_{end}$ = last 10 trials in force field before tracking task; FFt_{end} = last 10 trials in tracking task; $FF2_{end}$ = last 10 trials in force field after tracking task; max *x*-dev = maximal *x*-deviation of the hand; v_{max} = maximal hand velocity. *Significant *P* value.

addition, in *experiment* 2 subjects could easily produce movements similar to the minimal energy path that required significantly less energy than that of the straight hand paths. Finally, due to the nature of the force field, subjects did not need to move along the minimal energy path that required a kinematic detour to reduce the energy cost; any small adjustment of their hand path to the right would do so (see also Fig. 1*B*). During their normal movement variability in the force field, subjects experience substantially different energy cost values (see Fig. 4*B*). However, despite having experienced paths requiring less energy as part of their normal variability in movement paths, subjects did not adapt their hand paths, not even after prolonged practice trials.

Arguably, one might suggest that energy is not minimized because the change in energy cost experienced during the trial-to-trial variability is too small. To assess this, we plotted a histogram of the calculated energy cost of every successful trial in the first experiment, minus the mean energy cost and normalized for the mean energy cost in the null field (ΔE; Fig. 6). In other words, ΔE is the change in energy cost experienced over different trials, expressed relative to the mean energy cost of moving in the null field. This figure shows that within their normal movement variability in the force field (±1SD), subjects experience a range in energy cost that is about 3.2-fold the energy it costs for them to move in the null field. This means that if subjects are not minimizing energy cost for arm movements in this force field because of small experienced differences in energy cost, this would be all the more true for movements in a null field (or free space).

In this study, we changed the minimal energy hand path of planar 2df reaching movements. As stated earlier, because subjects did not change their hand paths at all this must mean that energy expenditure is very unlikely to substantially contribute to adaptive motor control, at least in planar arm movements. In our opinion, this result also implies that it is improbable—but not impossible—that for more complex arm movements the CNS would minimize energy cost. This claim is supported by an experimental study of Flanders et al. (2003) that measured three-dimensional (3D) whole arm pointing movements while holding onto a gyroscope that introduced complex dynamics. It was found that subjects gradually returned to movements similar to those in free space and, from their analyses, it was concluded that the observed gradual change in movement patterns did not lead to significant changes in peak kinetic energy. A similar conclusion was reached by Hermens and Gielen (2004): model simulations in which peak mechanical work was minimized were not in agreement with experimental data on 3D reaching movements in free space. Nevertheless, it remains to be established that for more complex movements, such as 3D movements under the influence of gravity, the CNS does not minimize energy to acquire new muscle activation patterns.

The results of this study are in contradiction with previous work proposing that minimization of energy, or related variables, underlies the specification of kinematic features of reaching movements in several environments (e.g., Alexander 1997; Cruse 1986; Hatze and Buys 1977; Rasmussen et al. 2001; Soechting et al. 1995). As explained in METHODS, for movements in free space and, for example, in

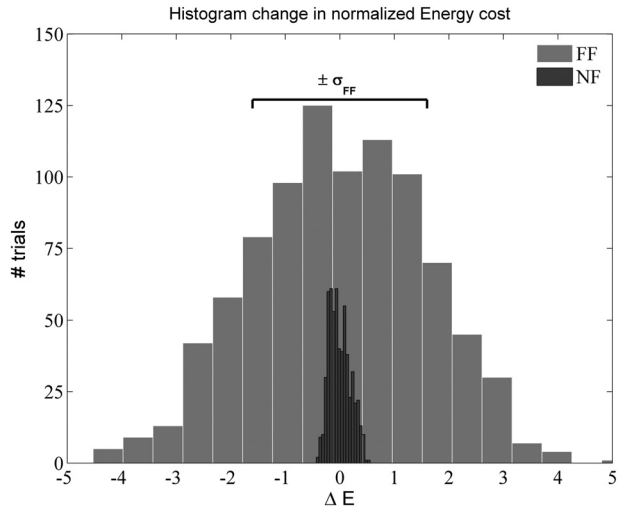

FIG. 6. Histogram of change in energy experienced over trials. The change in energy (ΔE) was calculated by subtracting the energy cost per trial from the mean energy cost and dividing by the mean energy cost to move in the null field. The depicted range denoted by $\pm\sigma_{FF}$ equals ±1SD of the energy cost in the force field normalized for the mean energy cost in the null field. Included are all successful trials in the first experiment. Energy cost in the null and force fields, respectively: 0.34 J (±0.07) and 5.41 J (±0.55).

the often studied curl field (a force field for which the forces applied to the hand are perpendicular and proportional to the velocity of the hand; e.g., see Caithness et al. 2004), minimal energy paths are essentially the same (relatively straight hand paths). Thus such conditions are not adequate to investigate whether energy minimization actually takes part in acquiring new motor skills. On the other hand, the main result of this study is not necessarily at odds with studies that suggest that tasks like walking and running (Alexander 1991; Margaria 1976; Zarrugh and Radcliffe 1978) are, under normal circumstances, performed in an energetically efficient way. Although the present results suggest that such minimization of energy cost is not under the immediate control of the CNS, it is quite possible, for example, that energetic cost of movements has decreased over a long timescale due to evolutionary pressure. The results of this study raise the question: If energy cost is not a dominant factor in adaptive control of reaching movements, what is? Other factors like stability (Balasubramanian et al. 2009), control effort (Todorov and Jordan 2002), and minimizing (endpoint) variance due to signal-dependent noise (Harris and Wolpert 1998) are candidates for further research.

APPENDIX: MUSCLE MODEL AND METABOLIC ENERGY EXPENDITURE MODEL

Muscle model

ACTIVATION DYNAMICS. Activation dynamics was modeled according to Hatze (1977; see also Kistemaker et al. 2005) and related muscle stimulation (*STIM*) to active state (q) in two steps. A first-order dynamic system related the free Ca^{2+} concentration (relative to its maximum value; γ_{rel}) to *STIM*. Subsequently, an algebraic relation described how active state q depends on γ_{rel} and (via ρ) on *CE* length relative to its optimum at maximal q (l_{CE_rel})

$$\dot{\gamma}_{rel} = m \cdot (STIM - \gamma_{rel}) \quad \text{(A1)}$$

$$q = \frac{q_0 + (\rho \cdot \gamma_{rel})^3}{1 + (\rho \cdot \gamma_{rel})^3} \quad \text{(A2)}$$

where ρ is a function of l_{CE_rel}

$$\rho = c \cdot \eta \ \frac{(k-1)}{(k - l_{CE\_rel})} \ l_{CE\_rel} \quad \text{(A3)}$$

where η, k, c, m, and q_0 are constants (see Table A1).

The original equations of Hatze are simplified for clarity. For a graphical representation of the *STIM*–q relationship as a function of l_{CE_rel}, see Fig. A1*A*. It was previously shown that this model of activation dynamics is capable of adequately describing the shifts in optimum l_{CE} at submaximal muscle stimulations (Kistemaker et al. 2005).

TABLE A1. *Muscle nonspecific parameters*

Parameter	Value	Parameter	Value
m	11.30	$width$	0.66
c	1.37e-4	a_{rel}	0.41
η	5.27e4	b_{rel}	5.20
q_0	5.00e-3	q_{crit}	0.03
k	2.90		

CONTRACTION DYNAMICS. Contraction dynamics was modeled by relating the contraction velocity (v_{CE}) to l_{CE}

$$v_{CE} = f(l_{CE}, q, \varphi) \quad \text{(A4)}$$

The contraction velocity was derived from the difference between the isometric force (F_{isom}), calculated using the force–length relationship, and the actual force to be generated by the *CE* (F_{CE}). Assuming that the mass of the muscle was negligible with respect to the force it is producing, F_{CE} equaled the difference between the force of *SE* (F_{SE}) and that of *PE* (F_{PE}). The concentric ($v_{CE} < 0$ or $F_{CE} < F_{isom}$) and eccentric ($v_{CE} > 0$ or $F_{CE} > F_{isom}$) parts of the force–velocity relationship were modeled separately. The concentric part was described based on the classic Hill equation, which was solved for v_{CE_rel} (the time derivative of l_{CE_rel})

$$v_{CE\_rel} = \frac{b^*_{rel}(F_{CE\_rel} - q \cdot F_{isom\_n})}{F_{CE\_rel} + q \cdot a^*_{rel}} \quad \text{(A5)}$$

where $F_{CE\_rel} = F_{CE}/F_{MAX}$ and $F_{isom\_n} = F_{isom}/F_{MAX}$. Based on experimental results (Stern Jr 1974), maximal contraction velocity was made dependent on F_{isom_n} by setting: $a^*_{\mathrm{rel}} = a_{\mathrm{rel}} \cdot F_{\mathrm{isom\_n}}$ when $l_{CE} > l_{CE\_opt}$ and $a^*_{\mathrm{rel}} = a_{rel}$ when $l_{CE} \leq l_{CE\_opt}$. Furthermore, based on experimental results of Petrofsky and Phillips (1981) for low values of q, maximal contraction velocity was made dependent on q by setting

$$b^*_{rel} = b_{rel}\left[1 - 0.9\left(\frac{q - q_{crit}}{q_0 - q_{crit}}\right)^2\right] \quad \text{(A6)}$$

where $q < q_{crit}$ and $b^*_{\mathrm{rel}} = b_{rel}$ when $q \geq q_{crit}$. Values for the constants a_{rel}, b_{rel}, and q_{crit} are given in Supplemental Table S1.[1]

The eccentric part of the force–velocity relationship was modeled using a hyperbola. To prevent numerical problems, a hyperbola with a slightly slanted asymptote was used (for the sake of conciseness, it was not solved here for v_{CE_rel})

$$(F_{CE\_rel} + p_3 + p_4 \cdot v_{CE\_rel})(v_{CE\_rel} + p_1) = p_2 \quad \text{(A7)}$$

The parameters p_1, p_2, p_3, and p_4 were calculated using four criteria: *1*) the concentric and eccentric curve are continuous; *2*) based on Katz (1939), the derivative of F_{CE_rel} with respect to v_{CE_rel} at $v_{CE\_rel} = 0$ of the eccentric curve was twice that of the concentric curve; *3*) the asymptote had a value of $1.5q \cdot F_{isom\_n}$ at $v_{CE\_rel} = 0$; and *4*) and arbitrary small value for the slope of the asymptote. Note that the calculated parameters were functions of F_{isom_n} such that both parts of the force–velocity relationship depended on F_{isom_n} and F_{CE_rel}. See Supplemental Fig. S2, *C* and *D* for a graphical representation of the force–velocity relationship at different values of q and l_{CE_rel}.

Normalized isometric force (F_{isom_n}) was modeled as a second-order polynomial with an optimum at $l_{CE\_rel} = 1$ and two zero-crossings at $l_{CE\_rel} = 1 \pm width$

$$F_{isom\_n} = -a \cdot l^2_{CE\_rel} + 2a \cdot l_{CE\_rel} - a + 1 \quad \text{(A8)}$$

where $a = 1/width^2$. For a graphical representation of the isometric force–length–stimulation relation, see Fig. A1*B*.

[1] The online version of this article contains supplemental data.

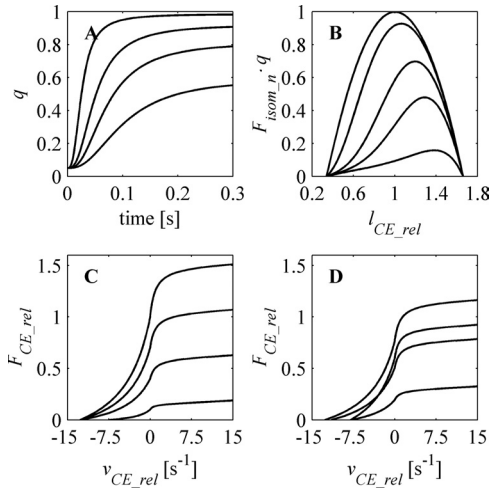

FIG. A1. *A*: $q(t)$ for $STIM = 0.3$ and $l_{CE\_rel} = 0.6, 0.8, 1.0, 1.4$ (longer l_{CE_rel} = higher q). *B*: isometric force–length characteristic for $STIM = 0.05, 0.1, 0.15, 0.3, 1$ (higher $STIM$ = higher force). *C*: force–velocity characteristic for $l_{CE\_rel} = 1.0$ and $q = 0.1, 0.4, 0.7, 1.0$ (higher $STIM$ = higher F_{CE_rel}). Note that at $q < 0.3$, maximal shortening velocity scales with q. *D*: force–velocity characteristic for $STIM = 0.2$ and $l_{CE\_rel} = 1.0, 1.4, 0.8, 0.6$ (in order of highest maximal F_{CE_rel}). Note that at $l_{CE\_rel} > 1$, maximal shortening velocity scales with F_{isom_n}. Maximal shortening velocity of the lower force–velocity characteristic in *D* is diminished because at this $STIM$ and l_{CE_rel}, q is <0.3 (see *C*).

The passive force–length characteristic of the PE was modeled to depend quadratically on l_{CE_rel} (note that $l_{PE} = l_{CE}$)

$$F_{PE} = k_{PE} \cdot \left[\max\left(0, l_{CE\_rel} - \frac{l_{PE\_0}}{l_{CE\_opt}}\right)\right]^2 \quad \text{(A9)}$$

where $l_{PE\_0} = 1.4 l_{CE\_opt}$ and k_{PE} was chosen such that $F_{PE} = F_{MAX}$ at $l_{CE\_rel} = 1 + width$. The passive force characteristic of the *SE* was modeled to depend quadratically on l_{SE}

$$F_{SE} = k_{SE} \cdot \left[\max\left(0, l_{SE} - l_{SE\_0}\right)\right]^2 \quad \text{(A10)}$$

k_{SE} was chosen such that at F_{MAX} *SE* is at 104% of l_{SE_0}. For a graphical representation of the force–length relationships of the elastic components see Fig. A1, *A* and *B*. The muscle parameters F_{MAX}, l_{SE_0}, and l_{CE_opt} were obtained from the literature (Murray et al. 1995, 2000; Nijhof and Kouwenhoven 2000). F_{SE} and F_{PE} were calculated using the muscle tendon complex length (l_{MTC}) and l_{CE}. Parameter values are listed in Table A2.

l_{MTC} was modeled as a second-order polynomial depending on elbow (φ_e) and shoulder angle (φ_s)

$$l_{MTC}(\varphi_e, \varphi_s) = a_0 + a_{1e}\varphi_e + a_{2e}\varphi_e^2 + a_{1s}\varphi_s \quad \text{(A11)}$$

Values of a_{1e}, a_{2e}, and a_{1s} were based on cadaver data literature (Murray et al. 1995, 2000; Nijhof and Kouwenhoven 2000), obtained using the tendon displacement method (see Grieve et al. 1978); values for a_0 representing l_{MTC} at $\varphi_e = \varphi_s = 0$ (and *width*; see *Eq.* A*11*) were chosen such that the optimum angle for maximal isometric moment was consistent with the literature (Kistemaker et al. 2007a). Moment arms were calculated by taking the partial derivative of l_{MTC} to φ_e and φ_s

$$arm_e(\varphi_e) = \frac{\partial l_{MTC}}{\partial \varphi_e} = a_{1e} + 2a_{2e}\varphi_e \quad \text{(A12)}$$

$$arm_s(\varphi_s) = \frac{\partial l_{MTC}}{\partial \varphi_s} = a_{1s} \quad \text{(A13)}$$

Energy expenditure model

Umberger's energy expenditure model was previously explained and described in full detail elsewhere (Umberger et al. 2003). The variables used in this model are identical to those used in the musculoskeletal model. A brief description of the full model is in the following text; note that the formulation and naming are slightly reformatted for convenience.

The total metabolic energy was calculated by integrating the following rate of metabolic energy liberation ($\dot{E}_{met}$) term

$$\dot{E}_{met} = \dot{h}_{AM} + \dot{h}_{SL} + \dot{w}_{CE} \quad \text{(A14)}$$

where $\dot{h}_{AM}$ is the activation/maintenance heat, $\dot{h}_{SL}$ is the shortening/lengthening heat, and $\dot{w}_{CE}$ is the rate of work done by the CE.

$\dot{h}_{AM}$ is linearly related to the percentage of fast twitch fibers (%FT, data obtained from Dahmane et al. 2005; Johnson et al. 1973; see Supplemental Table S2)

$$\begin{aligned} \dot{h}_{AM} &= A_{AM} \cdot S(1.28 \cdot \%\text{FT} + 25) \\ &\quad \text{when } l_{CE} \le L_{CE\_opt} \\ \dot{h}_{AM} &= A_{AM} \cdot S(1.28 \cdot \%\text{FT} + 25) \cdot (0.4 + 0.6F_{ISO}) \\ &\quad \text{when } l_{CE} > L_{CE\_opt} \end{aligned} \quad \text{(A15)}$$

where

$$S = 1.25$$

$$\begin{aligned} A_{AM} &= STIM^{0.6} \quad \text{when } STIM > q \\ A_{AM} &= (STIM + q)^{0.6} \quad \text{when } STIM \le q \end{aligned}$$

$\dot{h}_{SL}$ depends on the muscle type, on the shortening (α_{S_ST} and α_{S_FT}) and lengthening heat coefficient (α_L), and on the relative contraction velocity (v_{CE_rel}). For shortening ($v_{CE\_rel} \le 0$)

TABLE A2. *Muscle-specific parameters*

Muscle	F_{MAX}, N	l_{CE_opt}, m	l_{SE_0}, m	l_{PE_0}, m	a_0, m	a_{1e}, m	a_{1s}, m	a_{2e}, m	%FT, %
MEF	1,422	0.092	0.172	0.129	0.286	−0.014	0.0	−3.96e-3	50.3
MEE	1,549	0.093	0.187	0.130	0.236	0.025	0.0	−2.16e-3	42.9
BEF	414	0.137	0.204	0.192	0.333	−0.016	−0.030	−5.73e-3	54.5
BEE	603	0.127	0.217	0.178	0.299	−0.014	0.030	−3.18e-3	64.7
MSF	838	0.134	0.039	0.187	0.151	0.0	0.030	0.0	53.6
MSE	1,207	0.140	0.066	0.196	0.232	0.0	−0.030	0.0	64.7

MEF, monoarticular elbow flexor; BEE, biarticular elbow extensor.

$$\dot{h}_{SL} = -\alpha_{S\_ST} \cdot v_{CE\_rel}(1 - \%FT/100) - \alpha_{S\_FT} \cdot v_{CE\_rel}(\%FT/100) \quad (A16a)$$

where

$$\alpha_{S\_ST} = \frac{100}{v_{CE\max ST}} \quad \alpha_{S\_FT} = \frac{153}{v_{CE\max FT}}$$

and for lengthening ($v_{CE\_rel} > 0$)

$$\dot{h}_{SL} = \alpha_L \cdot v_{CE\_rel} \cdot A \cdot S \quad \text{when } l_{CE} \le L_{CE\_opt}$$
$$\dot{h}_{SL} = \alpha_L \cdot v_{CE\_rel} \cdot A \cdot S \cdot F_{isom} \quad \text{when } l_{CE} > L_{CE\_opt} \quad (A16b)$$

where

$$\alpha_L = \dot{h}_{SL} = 4\alpha_{S\_ST}$$

$\dot{w}_{CE}$ is the rate of work done by a muscle scaled with its mass (m)

$$\dot{w}_{CE} = -\frac{F_{CE} \cdot v_{CE}}{m} \quad (A17)$$

The state derivatives of the metabolic energy expenditure model are numerically integrated for each time step together with those of the musculoskeletal model described earlier.

Muscle activation patterns

Muscle activation patterns were found by optimizing the following cost function

$$J = k_1(p_{des} - p_{end})^2 + k_2\dot{p}_{end}^2 + k_3\ddot{p}_{end}^2 + k_4E_{met} \quad (A18)$$

where k_{1-4} represents the optimization parameters; p_{des} is the desired endpoint of the hand; p, $\dot{p}_{end}$, and $\ddot{p}_{end}$ represent the end position, velocity, and acceleration of the hand; and E_{met} is the metabolic energy spent by the muscles. In the case of a simulated force field, forces at the hand of the musculoskeletal model were added that were identical to the commanded forces to the robot manipulandum. Muscle activation patterns were found by numerical optimization using a Trust–Region–Reflective constraint optimization implemented in MATLAB.

GRANTS

This work was supported by grants from the Natural Sciences and Engineering Research Council of Canada and the Canadian Institutes of Health Research (CIHR). D. A. Kistemaker was supported by The Netherlands Organisation for Scientific Research. J. D. Wong was supported by a Canada Graduate Scholarship from CIHR.

DISCLOSURES

No conflicts of interest, financial or otherwise, are declared by the author(s).

REFERENCES

Abbate F, De Ruiter CJ, Offringa C, Sargeant AJ, De Haan A. In situ rat fast skeletal muscle is more efficient at submaximal than at maximal activation levels. *J Appl Physiol* 92: 2089–2096, 2002.

Alexander RM. Energy-saving mechanisms in walking and running. *J Exp Biol* 160: 55–69, 1991.

Alexander RM. A minimum energy cost hypothesis for human arm trajectories. *Biol Cybern* 76: 97–105, 1997.

Balasubramanian R, Howe RD, Matsuoka Y. Task performance is prioritized over energy reduction. *IEEE Trans Biomed Eng* 56: 1310–1317, 2009.

Bernstein N. *The Coordination and Regulation of Movements*. Oxford, UK: Pergamon, 1967.

Caithness G, Osu R, Bays P, Chase H, Klassen J, Kawato M, Wolpert DM, Flanagan JR. Failure to consolidate the consolidation theory of learning for sensorimotor adaptation tasks. *J Neurosci* 24: 8662–8671, 2004.

Cruse H. Constraints for joint angle control of the human arm. *Biol Cybern* 54: 125–132, 1986.

Dahmane R, Djordjevic S, Simunic B, Valencic V. Spatial fiber type distribution in normal human muscle histochemical and tensiomyographical evaluation. *J Biomech* 38: 2451–2459, 2005.

d'Avella A, Portone A, Fernandez L, Lacquaniti F. Control of fast-reaching movements by muscle synergy combinations. *J Neurosci* 26: 7791–7810, 2006.

Engelbrecht SE. Minimum principles in motor control. *J Math Psychol* 45: 497–542, 2001.

Flanders M, Hondzinski JM, Soechting JF, Jackson JC. Using arm configuration to learn the effects of gyroscopes and other devices. *J Neurophysiol* 89: 450–459, 2003.

Flash T, Hogan N. The coordination of arm movements: an experimentally confirmed mathematical model. *J Neurosci* 5: 1688–1703, 1985.

Grieve DW, Pheasant S, Cavanagh PR. Prediction of gastrocnemius length from knee and ankle joint posture. In: *Biomechanics VI-A* (International Series on Biomechanics), edited by Asmussen E, Jorgensen K. Baltimore, MD: University Park Press, 1978, vol. 2A, p. 405–412.

Harris CM, Wolpert DM. Signal-dependent noise determines motor planning. *Nature* 394: 780–784, 1998.

Hatze H. A myocybernetic control model of skeletal muscle. *Biol Cybern* 25: 103–119, 1977.

Hatze H, Buys JD. Energy-optimal controls in the mammalian neuromuscular system. *Biol Cybern* 27: 9–20, 1977.

Hermens F, Gielen S. Posture-based or trajectory-based movement planning: a comparison of direct and indirect pointing movements. *Exp Brain Res* 159: 340–348, 2004.

Johnson MA, Polgar J, Weightman D, Appleton D. Data on the distribution of fibre types in thirty-six human muscles. An autopsy study. *J Neurol Sci* 18: 111–129, 1973.

Kashima T, Isurugi Y. Trajectory formation based on physiological characteristics of skeletal muscles. *Biol Cybern* 78: 413–422, 1998.

Katz B. The relation between force and speed in muscular contraction. *J Physiol* 96: 45–64, 1939.

Kistemaker DA, Van Soest AK, Bobbert MF. Length-dependent [Ca^{2+}] sensitivity adds stiffness to muscle. *J Biomech* 38: 1816–1821, 2005.

Kistemaker DA, Van Soest AJ, Bobbert MF. Is equilibrium point control feasible for fast goal-directed single-joint movements? *J Neurophysiol* 95: 2898–2912, 2006.

Kistemaker DA, Van Soest AJ, Bobbert MF. A model of open-loop control of equilibrium position and stiffness of the human elbow joint. *Biol Cybern* 96: 341–350, 2007a.

Kistemaker DA, Van Soest AK, Bobbert MF. Equilibrium point control cannot be refuted by experimental reconstruction of equilibrium point trajectories. *J Neurophysiol* 98: 1075–1082, 2007b.

Margaria R. *Biomechanics and Energetics of Muscular Exercise*. Oxford, UK: Clarendon Press, 1976.

Murray WM, Buchanan TS, Delp SL. The isometric functional capacity of muscles that cross the elbow. *J Biomech* 33: 943–952, 2000.

Murray WM, Delp SL, Buchanan TS. Variation of muscle moment arms with elbow and forearm position. *J Biomech* 28: 513–525, 1995.

Nelson WL. Physical principles for economies of skilled movements. *Biol Cybern* 46: 135–147, 1983.

Nijhof E, Kouwenhoven E. Simulation of multijoint arm movements. In: *Biomechanics and Neural Control of Posture and Movement*, edited by Winters J, Grago P. New York: Springer, 2000, p. 363–372.

Petrofsky JS, Phillips CA. The influence of temperature initial length and electrical activity on the force-velocity relationship of the medial gastrocnemius muscle of the cat. *J Biomech* 14: 297–306, 1981.

Rasmussen J, Damsgaard M, Voigt M. Muscle recruitment by the min/max criterion: a comparative numerical study. *J Biomech* 34: 409–415, 2001.

Soechting JF, Buneo CA, Herrmann U, Flanders M. Moving effortlessly in three dimensions: does Donders' law apply to arm movement? *J Neurosci* 15: 6271–6280, 1995.

Stern JT Jr. Computer modelling of gross muscle dynamics. *J Biomech* 7: 411–428, 1974.

Todorov E. Optimality principles in sensorimotor control. *Nat Neurosci* 7: 907–915, 2004.

Todorov E, Jordan MI. Optimal feedback control as a theory of motor coordination. *Nat Neurosci* 5: 1226–1235, 2002.

Torres EB, Zipser D. Reaching to grasp with a multi-jointed arm. I. Computational model. *J Neurophysiol* 88: 2355–2367, 2002.

Umberger BR, Gerritsen KG, Martin PE. A model of human muscle energy expenditure. *Comput Methods Biomech Biomed Eng* 6: 99–111, 2003.

Uno Y, Kawato M, Suzuki R. Formation and control of optimal trajectory in human multijoint arm movement. Minimum torque-change model. *Biol Cybern* 61: 89–101, 1989.

Zarrugh MY, Radcliffe CW. Predicting metabolic cost of level walking. *Eur J Appl Physiol Occup Physiol* 38: 215–223, 1978.

Zarrugh MY, Todd FN, Ralston HJ. Optimization of energy expenditure during level walking. *Eur J Appl Physiol Occup Physiol* 33: 293–306, 1974.